Activity Driven Orientational Order in Active Nematic Liquid Crystals on an Anisotropic Substrate

D. J. G. Pearce
Department of Theoretical Physics, University of Geneva, Geneva, Switzerland
and Department of Biochemistry, University of Geneva, Geneva 1205, Switzerland

(Received 11 September 2018; published 7 June 2019)

We investigate the effect of an anisotropic substrate on the turbulent dynamics of a simulated two-dimensional active nematic. This is introduced as an anisotropic friction and an effective anisotropic viscosity, with the orientation of the anisotropy being defined by the substrate. In this system, we observe the emergence of global nematic order of topological defects that is controlled by the degree of anisotropy in the viscosity and the magnitude of the active stress. No global defect alignment is seen in passive liquid crystals with anisotropic viscosity or friction confirming that ordering is driven by the active stress. We then closely examine the active flow generated by a single defect to show that the net kinetic energy of the flow is dependent on the orientation of the defect relative to the substrate, resulting in a torque on the defect to align it with the anisotropy in the substrate.

DOI: 10.1103/PhysRevLett.122.227801

Active nematics are fluids consisting of self- (or mutually) propelling rod shaped particles resulting in an anisotropic fluid with broken rotational symmetry that drives itself at the microscopic scale [1–5]. This combination of broken rotational symmetry and out of equilibrium, active behavior has led to an explosion of interest from both experimental and theoretical physics [1,2,6–9]. There have been many successful experiments reproducing active nematics often utilizing biological components, including microtubule kinesin suspensions [1,2,10] and elongated cells [11–14], but also from inert components such as vibrated monolayers of granular rods [15]. Active polar liquid crystals have also been experimentally realized using actomyosin gels [16,17].

These systems display a rich phenomenology depending on many factors such as the degree to which the system is driven [7], the confining geometry [18], the density [13], and the boundary conditions [19]. By varying these factors it is possible to observe diverse spatiotemporal patterns including vortices [14,18], oscillating textures [16,20], and traveling bands [16,18]. When the driving force is sufficiently high, active nematics can spontaneously nucleate many topological defects, generating flows and interacting chaotically in a regime referred to as low Reynolds number, active turbulence [1,7,11,21]. These defects have been shown to exert elastic and hydrodynamic torques on each other [22–26], and experiments have indicated that long range nematic order of defects is possible in a state of active turbulence [27] though this has not yet been reproduced theoretically. It has been shown that the position and orientation of these defects can be influenced by the substrate on which the active nematic is placed. By changing the geometry of the substrate it is possible to reorient defects and sort them by charge [28], and by changing the topology of the substrate it is possible to control the total number of defects and their trajectories [20]. A defect ordered active nematic has been recreated by placing a two-dimensional (2D) active nematic on top of a passive liquid crystal that can be controlled by an external magnetic field [29]. When the passive liquid crystal layer is ordered into a smectic state by the magnetic field, it creates a global anisotropy, defined by the orientation of the director in the passive liquid crystal. When the two layers are in contact, the passive liquid crystal layer acts as an anisotropic dissipative agent for the flows generated in the driven active layer. As a result, the active nematic layer forms antiparallel channels containing ordered topological defects [29].

In this Letter, we explore how the introduction of anisotropic dissipative forces can lead to activity driven order in a simulated turbulent active nematic. First, we define a general viscosity and friction for a standard continuum model for active nematics in two dimensions. We then introduce the anisotropy to these quantities based on the substrate frame of reference. We observe that the active stress drives global nematic alignment of defects in the presence of anisotropic viscosity but not anisotropic friction. This global nematic order depends on the degree of anisotropy in the viscosity and the degree to which the active nematic is driven. We then support the hypothesis that this ordering is an active process by simulating passive liquid crystals with anisotropic viscosity which displays no such ordering. Finally, we analyze the flow patterns around a single defect, noting that the energy dissipation of the active flows induces an active torque on the defects.

We start from the generic form of the equations governing an incompressible active nematic which are given by

$$\rho\partial_t v_i = \partial_j \sigma_{ij}^{(t)} - \partial_j p\delta_{ij} - \mu_{ij} v_j, \tag{1}$$

$$[\partial_t + v_i\partial_i]Q_{ij} = \lambda S u_{ij} + Q_{ik}\omega_{kj} - \omega_{ik}Q_{kj} + \gamma^{-1}H_{ij}, \tag{2}$$

where ρ is the density, $\sigma_{ij}^{(t)}$ is the total stress tensor, and the tensor μ_{ij} contains the friction coefficients. Because we are considering the incompressible limit, $\partial_i v_i = 0$ and $\rho = 1$ everywhere. $Q_{ij} = S(n_i n_j - \delta_{ij}/2)$ is the nematic tensor, S is the nematic order parameter, and λ is the flow alignment parameter. The strain rate tensor is given by $u_{ij} = (\partial_i v_j + \partial_j v_i)/2$, vorticity tensor $\omega_{ij} = (\partial_i v_j - \partial_j v_i)/2$, and molecular tensor $H_{ij} = -\partial F/\partial Q_{ij}$ where F is the Landau–de Gennes free energy, and in two dimensions is given by

$$F = \frac{K}{2}\int dA\left(|\nabla Q|^2 + \frac{1}{\epsilon^2}\mathrm{tr}Q^2(\mathrm{tr}Q^2 - 1)\right), \tag{3}$$

where the parameter ϵ is a characteristic length, which is proportional to the core defect radius, and K is the elastic constant associated with distortions in the director field. The cubic term is not included here as in a 2D system it is identically zero. Previous experiments on active nematics influenced by anisotropic substrates have considered microtubule-based active nematics on a substrate of octyl-cyanobiphenyl (8CB) [29]. In such a system, we expect any nematic anchoring between the two layers to be very small due to the large difference in length scale between the microtubules (∼25 nm diameter) and the 8CB (∼1 nm length). For this reason, we assume no surface anchoring in Eq. (3).

The total stress tensor ($\sigma^{(t)}$) is the sum of elastic stresses ($\sigma^{(e)}$), viscous stresses ($\sigma^{(v)}$), and the active stress generated by the molecular motors ($\sigma^{(a)}$) controlled by parameter α. In the general form, these stress tensors are given by

$$\sigma_{ij}^{(e)} = -\lambda S H_{ij} + Q_{ik}H_{kj} - H_{ik}Q_{kj}, \tag{4}$$

$$\sigma_{ij}^{(v)} = \nu_{ijkl}\partial_k v_l, \tag{5}$$

$$\sigma_{ij}^{(a)} = \alpha Q_{ij}. \tag{6}$$

We introduce the anisotropy through the viscous stress tensor and the friction tensor. Since this anisotropy is defined by the substrate, we must introduce an external frame of reference. Without loss of generality we assume that the high and low viscosity directions are aligned parallel to the x and y axes. With this condition we can assume the viscous stress tensor in two dimensions has the form

$$\sigma_{xx}^{(v)} = \nu_1\partial_x v_x, \tag{7}$$

$$\sigma_{xy}^{(v)} = (\nu_2\partial_x v_y + \nu_3\partial_y v_x)/2, \tag{8}$$

$$\sigma_{yx}^{(v)} = (\nu_4\partial_y v_x + \nu_5\partial_x v_y)/2, \tag{9}$$

$$\sigma_{yy}^{(v)} = \nu_6\partial_y v_y. \tag{10}$$

If at this stage we were to set all values of ν to be identical, we would obtain the normal viscous stress tensor for an isotropic fluid. Without loss of generality, we set $\nu_6 = \nu$. We make the further simplifying assumptions, allowed by symmetry for an incompressible fluid, that $\nu_3 = \nu_5 = \nu_1 = \nu$ and that $\nu_2 = \nu(1 - \Delta_\nu)$ and $\nu_4 = \nu(1 + \Delta_\nu)$ with the constraint $(0 \le \Delta_\nu \le 1)$. Here ν controls the magnitude of the isotropic viscosity, and the anisotropic contributions to the viscosity are controlled with the dimensionless parameter Δ_ν. When $\Delta_\nu \neq 0$ the dissipative effects of the perpendicular gradient of a flow are different depending on whether it is aligned with the x or y axis. This introduces an antisymmetric part to the viscous stress tensor, owing to the fact that the substrate is additionally serving as an angular momentum sink. It should be noted that the anisotropic viscosity that we have introduced here depends on an external frame of reference (the x and y axes); hence, it is no longer Galilean invariant [30]. The viscosity introduced here is that which would exist in a fully ordered incompressible nematic oriented parallel to the x axis [31], which is similar to the substrate used by Guillamat *et al.* [29]; see Supplemental Material [32] for details.

The anisotropic friction tensor can be defined generally as

$$\mu_{ij} = \mu^{(0)}\delta_{ij} + \mu_{ij}^{(1)}, \tag{11}$$

where μ_0 is the general isotropic substrate friction and μ_{ij} is the anisotropic part of the friction containing the required symmetries of the substrate. Since the friction tensor must be symmetric, it can be diagonalized by the correct choice of basis. We achieve this by choosing our friction asymmetry to align with our basis coordinates (the x and y axes). Therefore, the off diagonal components of the anisotropic friction tensor must be zero ($\mu_{xy}^{(1)} = \mu_{yx}^{(1)} = 0$), and we can define the anisotropic friction with two coefficients. We introduce the anisotropy in a similar fashion to the viscosity and set $\mu_{xx} = \mu_0(1 - \Delta_\mu)$ and $\mu_{yy} = \mu_0(1 + \Delta_\mu)$. This formulation allows us to control the degree of anisotropy fully by the dimensionless parameters $\Delta\nu$ and Δ_μ.

Equations (1) and (2) are simulated with a periodic boundary in two dimensions recreating an active nematic with varying degrees of anisotropy in either the viscosity or friction. The model parameters are selected such that the system is in a state of active turbulence containing of the

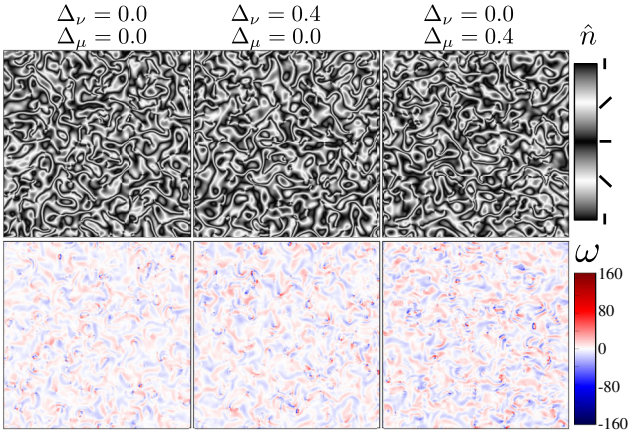

FIG. 1. Typical director (top) and vorticity (bottom) for an isotropic active nematic (left), an active nematic with anisotropic viscosity (middle) and anisotropic friction (right). The difference between the fields is not obvious; however, some short wavelength fluctuations in the y direction of the vorticity field are visible in the anisotropic viscosity case.

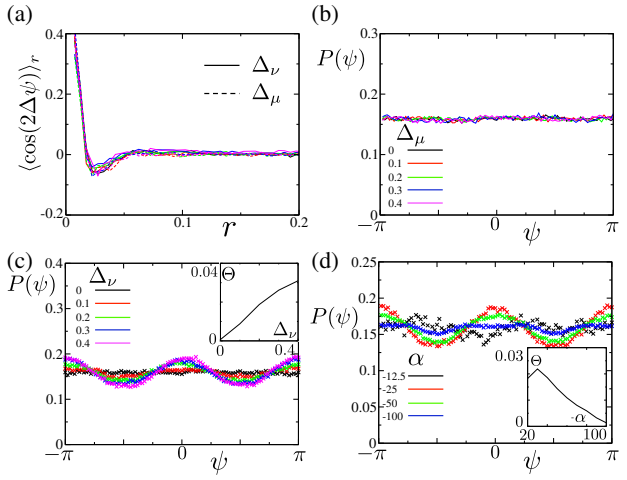

FIG. 2. (a) Nematic correlation function between positive defects. The location and depth of the minima are not significantly affected by the anisotropy, which implies that the active length scale and the elastic torques between defects are unaffected by the anisotropy. (b) Probability density function for the orientation of defects (ψ) within an active nematic with varying degrees of anisotropic friction (Δ_μ); there is no clear order in the defect orientations. (c) Probability density function for the orientation of defects within an active nematic with varying degrees of anisotropic viscosity (Δ_ν); a clear nematic order (Θ) is observed that increases with the degree of anisotropy (inset). (d) Global nematic order is not observed for very small or very large values of activity for fixed anisotropy ($\Delta_\nu = 0.3$). We can identify an apparent peak in the active stress (inset).

order of 200 defects; see Supplemental Material [32] for details. We choose to look at the influence of anisotropic viscosity and friction independently by either setting Δ_μ or Δ_ν to zero in all results presented here. Figure 1 shows the resulting director (top row) and vorticity (bottom row) of active nematics with isotropic hydrodynamics (left column), anisotropic viscosity (middle column), and anisotropic friction (right column). From these images it is very difficult to distinguish the nematic textures of each system. The vorticity fields show some signs of anisotropy, with some short wavelength fluctuations in the y direction being visible for the anisotropic viscosity system.

The lowest energy topological defects in a two-dimensional nematic have half integer charge, resulting in the characteristic $\pm 1/2$ defects that are regularly observed in active nematics. Since these defects are not rotationally symmetric, they have an easily defined orientation which we will annotate ψ. The angle of the director field (θ) around any of these defects can be expressed as $\theta = k(\phi - \psi) + \psi$, where ϕ is the polar angle between a reference axis (in this case the x axis) and the position around the defect core and k gives the charge of the defect [22]. We use this definition to measure the orientation, ψ, of all defects in the simulated nematic.

The nematic correlation function between positive defects is defined by $C_2(r) = \langle\cos[2(\psi_i - \psi_j)]\rangle_{i-j\sim r}$, shown in Fig. 2(a). Here we see that the orientational correlation length between defects is largely unaffected by the introduction of anisotropic friction or viscosity. The correlation length is set by the active length scale, given by $l_\alpha^2 \sim K/\alpha$. This is the length at which the active and elastic forces balance, and is proportional to the inter defect spacing [7,21]. The location of the minimum of the curve does not change; hence the introduction of anisotropic friction and viscosity does not affect the active length scale or the elastic torques that defects inflict upon each other.

The distribution of $+1/2$ defect orientations within a simulated active nematic with isotropic friction and viscosity in the turbulent regime is uniform; i.e., there is no global alignment of defects. The same is true for an active nematic with anisotropic friction [Fig. 2(b)]. However, for an active nematic with anisotropic viscosity, a clear nematic order emerges with positive defects being preferentially aligned parallel with the direction associated with the lowest viscosity [Fig. 2(c)]. We measure the magnitude of this order by fitting the histogram to the function $f(\psi) = 0.5/\pi + \Theta\cos(2\psi)$, allowing us to observe that the ordering is stronger with a more significant anisotropy; see Fig. 2(c) (inset). This emergent global order is mediated by the magnitude of the active stress, with the nematic ordering of the defects becoming reduced when the activity is either too high or too low [Fig. 2(d)]. These results suggest that the ordering of defects within an active nematic is related to the interaction between the flow generated by the defects and the anisotropic viscosity of the fluid. However, when the activity becomes very large, the alignment is lost [Fig. 2(d)] (inset).

In order to test the hypothesis that the active flow drives a global alignment, we perform a similar study in passive

nematic systems with anisotropic viscosity and friction. In the absence of an active stress, a passive nematic will relax toward the lowest energy state of the system, a uniform director field. If the nematic starts from an initially disordered state containing many defects, this process of minimizing the internal energy involves significant rearrangement of the director and the annihilation of many defects; see Fig. 3(a). This motion of the nematic generates a flow in the suspending fluid; see Fig. 3(b). The introduction of anisotropic friction or viscosity does not appear to affect this relaxation process of a passive nematic, with the number of defects in all samples decaying at a very similar rate [Fig. 3(c)]. By simulating many passive nematics from independent, random initial conditions for the same amount of time, it is possible to create many samples of a passive nematic all at the same stage of relaxation containing a similar number of defects. This approach can be used to study large numbers of interacting defects in passive nematics and has been used here to confirm no global nematic orientation of defects, even in cases with anisotropic friction or viscosity; see Fig. 3(d). These observations indicate that the hydrodynamic flows generated by elastic interactions alone are insufficient to generate any net defect ordering in our system.

The results presented in Figs. 2 and 3 indicate that the ordering of defects observed in active nematics is due to the interactions between the active flow and the anisotropic viscosity. The flow is generated by gradients in the nematic director and usually maximized around defects which generate characteristic flow patterns [7]. The positive defects generate strong polar flows which lead them to "swim" through the fluid giving them a self-propelled particlelike behavior. By simulating the flow field generated by a fixed nematic texture containing a single defect with a predetermined orientation, we can observe directly how the flow interacts with the anisotropic viscosity and friction. In an isotropic fluid, this is of course independent of the orientation of the defect; see Fig. 4(a) (top row). The introduction of anisotropic viscosity and friction distorts these flow patterns, as they adapt to the dissipative forces of the substrate; see Fig. 4(a) (middle and bottom rows, respectively). It is immediately apparent that when a defect is not aligned with either principal direction, the flow pattern around the defect loses its mirror symmetry in anisotropic cases [Fig. 4(a)] (middle column).

Figure 4(b) shows the net kinetic energy of the flow around a defect $E = \rho \int v^2 dA$. For the isotropic case, this is independent of defect orientation. When anisotropic viscosity or friction is introduced, we observe a clear

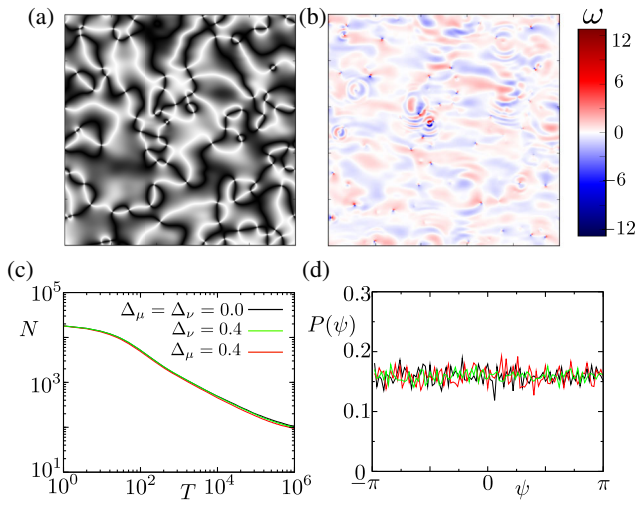

FIG. 3. Snapshot of a typical nematic director (a) and vorticity (b) at the point of measurement for a passive nematic with anisotropic viscosity. (c) Number of defects as a function of simulation time. The introduction of anisotropic hydrodynamics does not appear to affect the course graining dynamics. (d) Probability density function for the orientation of positive defects in a passive nematic at the point of measurement containing 96-104 total defects. We see no emergent global order.

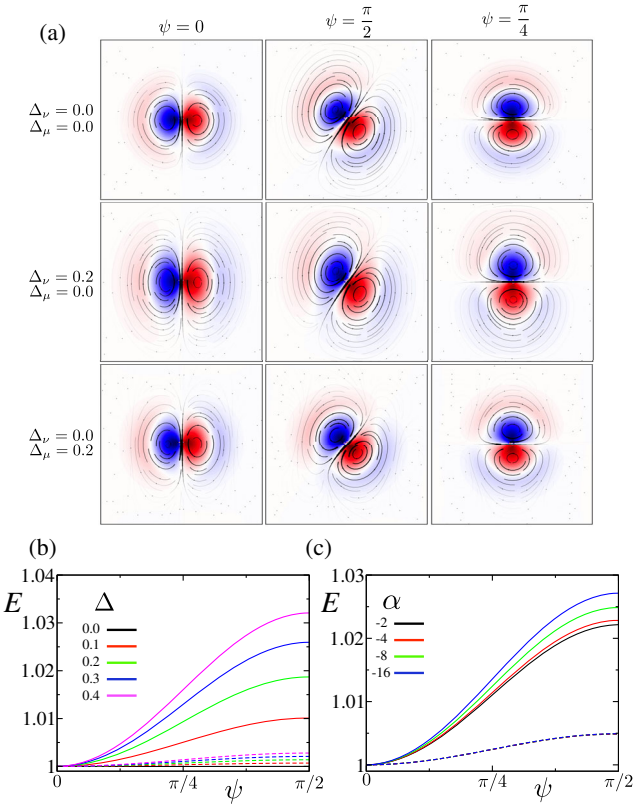

FIG. 4. (a) Flow pattern around a single positive defect for different orientations (column) and different anisotropies (row). We see that the mirror symmetry of flow around the defect core can be lost due to anisotropic viscosity or friction for certain orientations. (b) Kinetic energy (E) of the flow around each defect as a function of orientation for various degrees of anisotropy in either the viscosity (solid lines) or friction (dashed lines). (c) Kinetic energy of the flow around a defect for various values of activity (α) for systems with anisotropic viscosity (solid lines) and friction (dashed lines). Lowest energy configuration is always for the defect to be parallel with the x axis.

dependence of the net kinetic energy of the flow and the defect orientation, with the system being in a minimum energy configuration when the defect is aligned parallel to the direction of minimal shear viscosity $\psi = 0$. In both cases, the magnitude of the energy difference depends on the magnitude of the anisotropy Δ but is significantly larger for the anisotropic viscosity case [Fig. 4(b)]. As the active stress is increased, we see that the dependence of the energy on the defect orientation increases for systems with anisotropic viscosity, but not in cases with anisotropic friction [Fig. 4(c)]. This supports the hypothesis that the global ordering of defects is driven by activity.

In active nematics, the active stress drives the system toward "active turbulence," a chaotic state at low Reynolds number featuring many topological defects with no net order. This highlights a common feature, that the insertion of active stresses often acts to reduce order, in this case destroying the order of the nematic director and proliferating defects. When the viscosity of the active nematic has an anisotropy defined by an external frame of reference, in this case the substrate, the active flows can lead to the emergence of global nematic order of the topological defects driven by the active stress. This is evidenced by the fact that such order is not observed in systems with no active stress. Topological defects generate active flows in the fluid, the kinetic energy of which must be dissipated by the friction and viscosity of the fluid. When the fluid viscosity defined by the substrate is anisotropic, the rate of energy dissipation depends on the orientation of a defect relative to the substrate. This energy difference generates a torque on the core of the defect leading to a preferential orientation. This torque depends on the magnitude of the anisotropy and the active stress. However, the active stress also defines the interdefect spacing and the defect lifetime. When the active stress is increased, the interdefect spacing is reduced. This leads to a relative increase in the elastic torques the defects exert on each other, which eventually overcomes the ordering effects of the anisotropic viscosity. In the case of anisotropic friction, the active stress does not increase the torque on the defects, so when the system is in a state of active turbulence, the disordering effects of the activity outweigh the ordering effects of the anisotropic friction in all observed cases.

I would like to thank Calres Blanch-Mercader, Karsten Kruse, and Nicholas Ecker for insightful discussions. The author would like to thank the Swiss National Science Foundation for their financial support through the NCCR.

[1] T. Sanchez, D. N. Chen, S. J. DeCamp, M. Heymann, and Z. Dogic, Nature (London) **491**, 431 (2012).
[2] T. Surrey, F. Nedelec, S. Leibler, and E. Karsenti, Science **292**, 1167 (2001).
[3] A. Doostmohammadi, J. Ignés-Mullol, J. M. Yeomans, and F. Sagués, Nat. Commun. **9**, 3246 (2018).
[4] D. Needleman and Z. Dogic, Nat. Rev. Mater. **2**, 17048 (2017).
[5] M. C. Marchetti, J. F. Joanny, S. Ramaswamy, T. B. Liverpool, J. Prost, M. Rao, and R. A. Simha, Rev. Mod. Phys. **85**, 1143 (2013).
[6] L. Giomi, M. J. Bowick, X. Ma, and M. C. Marchetti, Phys. Rev. Lett. **110**, 228101 (2013).
[7] L. Giomi, Phys. Rev. X **5**, 031003 (2015).
[8] K. Kruse, J. F. Joanny, F. Jülicher, J. Prost, and K. Sekimoto, Phys. Rev. Lett. **92**, 078101 (2004).
[9] S. Ramaswamy, R. Aditi Simha, and J. Toner, Europhys. Lett. **62**, 196 (2003).
[10] P. Guillamat, J. Ignés-Mullol, and F. Sagués, Nat. Commun. **8**, 564 (2017).
[11] C. Blanch-Mercader, V. Yashunsky, S. Garcia, G. Duclos, L. Giomi, and P. Silberzan, Phys. Rev. Lett. **120**, 208101 (2018).
[12] J. Dunkel, S. Heidenreich, K. Drescher, H. H. Wensink, M. Bär, and R. E. Goldstein, Phys. Rev. Lett. **110**, 228102 (2013).
[13] Z. You, D. J. G. Pearce, A. Sengupta, and L. Giomi, Phys. Rev. X **8**, 031065 (2018).
[14] H. Wioland, E. Lushi, and R. E. Goldstein, New J. Phys. **18**, 075002 (2016).
[15] V. Narayan, S. Ramaswamy, and N. Menon, Science **317**, 105 (2007).
[16] V. Schaller, C. Weber, C. Semmrich, E. Frey, and A. R. Bausch, Nature (London) **467**, 73 (2010).
[17] V. Schaller and A. R. Bausch, Proc. Natl. Acad. Sci. U.S.A. **110**, 4488 (2013).
[18] S. A. Edwards and J. M. Yeomans, Europhys. Lett. **85**, 18008 (2009).
[19] L. Giomi and A. DeSimone, Phys. Rev. Lett. **112**, 147802 (2014).
[20] F. C. Keber, E. Loiseau, T. Sanchez, S. J. DeCamp, L. Giomi, M. J. Bowick, M. C. Marchetti, Z. Dogic, and A. R. Bausch, Science **345**, 1135 (2014).
[21] E. J. Hemingway, P. Mishra, M. C. Marchetti, and S. M. Fielding, Soft Matter **12**, 7943 (2016).
[22] A. Vromans and L. Giomi, Soft Matter **12**, 6490 (2016).
[23] X. Tang and J. V. Selinger, Soft Matter **13**, 5481 (2017).
[24] D. Cortese, J. Eggers, and T. B. Liverpool, Phys. Rev. E **97**, 022704 (2018).
[25] S. Shankar, S. Ramaswamy, M. C. Marchetti, and M. J. Bowick, Phys. Rev. Lett. **121**, 108002 (2018).
[26] X. Tang and J. V. Selinger, Soft Matter **15**, 587 (2019).
[27] S. J. DeCamp, G. S. Redner, A. Baskaran, M. F. Hagan, and Z. Dogic, Nat. Mater. **14**, 1110 (2015).
[28] P. W. Ellis, D. J. G. Pearce, Y.-W. Chang, G. Goldsztein, L. Giomi, and A. Fernandez-Nieves, Nat. Phys. **14**, 85 (2018).
[29] P. Guillamat, J. Ignés-Mullol, and F. Sagués, Proc. Natl. Acad. Sci. U.S.A. **113**, 5498 (2016).
[30] More correctly this should be referred to as a higher order friction term as it depends on the motion relative to the substrate orientation. However, due to its effect on the two-dimensional fluid, changing the coefficient of shear viscosity relative to orientation, we present it as an anisotropic viscosity.
[31] P. G. de Gennes and J. Prost, *The Physics of Liquid Crystals* (Clarendon Press, Oxford, 1995).
[32] See Supplemental Material at http://link.aps.org/supplemental/10.1103/PhysRevLett.122.227801 for a derivation of the anisotropic terms, simulation details and results pertaining to negative defects.